# *Supplementary Material*

## 1. Chemical constituents of Kunxinning Granules identified by UPLC/Q-TOF/MS

### 1.1 Preparation of Kunxinning Granule sample

Take 2 bags of Kunxinning Granules (KXN) and grind them into a uniform powder. Take an appropriate amount of powder and dissolve it with 50% methanol to make 20 mg/mL KXN sample solution.

### 1.2 Chromatographic condition

The chromatography was performed on ACQUITY UPLC BEHC18 (2.1 mm ×100 mm, 1.7 μm) column at 30℃ with mobile phase A consisting of 0.1% formic acid water and mobile phase B consisting of acetonitrile by gradient elution (0-3 min, 5%-10% B; 3~4 min, 10%~18%B; 4~10 min, 18~22%B; 10~13 min, 22%~24%B; 13~18 min, 24%-26% B; 18-20 min, 26%-28% B; 20~23 min, 28~45%B; 23~26 min, 45%~65%B; 26~29 min, 65%~95%B; 29~31 min, 95%~5%B), the flow rate was 0.3 mL • $min^{-1}$, and the sample size was 2 μL.

### 1.3 Mass spectrum condition

The ion source was electrospray ion source (ESI), the ion source temperature was 100℃. The desolvent temperature was 250℃, the desolvent gas flow rate was 600 L • $h^{-1}$. The atomizer pressure was set to 45 psig. The source offset voltage was 80 V, the cone hole voltage was 30 V, and the capillary voltage was 2.5 kV. The m/z scan range is set from 100 to 1500, using the positive and negative ion scan mode.

The chemical composition of KXN was analyzed by UPLC/Q-TOF-MS. The Base Peak Ion (BPI) of KXN in positive and negative ion mode is shown in Supplementary Figure S1.

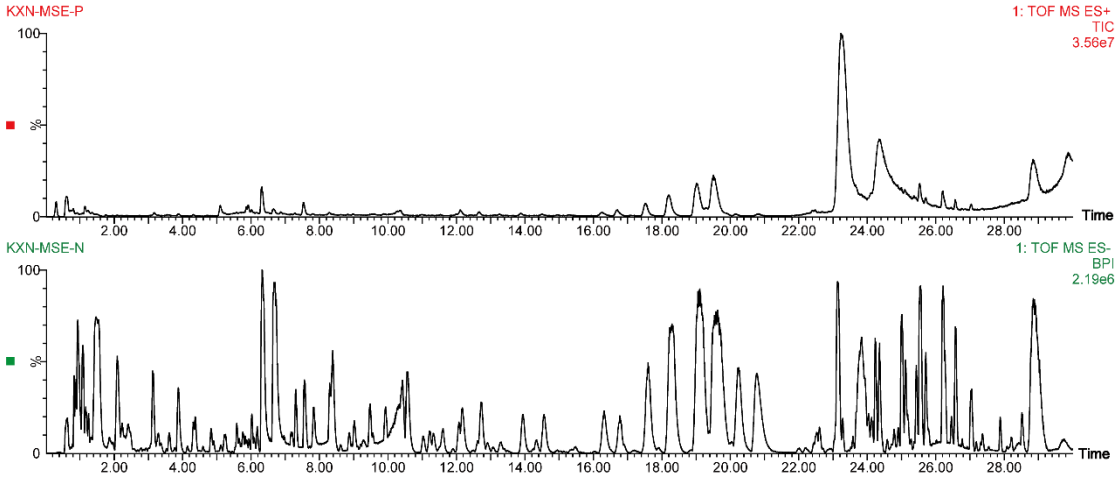


**Supplementary Figure S1.** BPI diagram of KXN UPLC/Q-TOF-MS in positive and negative ion mode.

According to database matching analysis, precise molecular weight, fragment ion peak and chromatographic retention time comparison, a total of 115 chemical components of KXN were identified, the specific information is shown in Supplementary Table S1. The mass spectras of each component based on UPLC/Q-TOF-MS are shown in supplementary data sheet S3.

**Supplementary Table S1.** Chemical components of KXN

| No. | $t_R$/min | Measured value | Precursor ions | Formula | Theoretical value | Compound | Fragment ion | CAS No. |
|---|---|---|---|---|---|---|---|---|
| 1 | 0.88 | 179.0573 | $[M-H]^-$ | $C_6H_{12}O_6$ | 179.0556 | Inositol | 160.9172 | 551-72-4 |
| 2 | 0.90 | 387.1156 | $[M-H]^-$ | $C_{17}H_{24}O_{10}$ | 387.1291 | Geniposide | 225.0657 | 24512-63-8 |
| 3 | 0.92 | 397.0942 | $[M-H]^-$ | $C_{22}H_{22}O_7$ | 397.1287 | Baohuosu | 397.0804, 259.0176, 191.0193 | 119730-90-4 |
| 4 | 1.42 | 191.0221 | $[M-H]^-$ | $C_6H_8O_7$ | 191.0192 | Citric acid | 173.0098, 129.0203 | 77-92-9 |
| 5 | 1.54 | 191.0193 | $[M-H]^-$ | $C_6H_8O_7$ | 191.0192 | Citric acid isomer | 173.0063, 129.0203, 111.0083 | - |
| 6 | 1.96 | 685.2255 | $[M-H]^-$ | $C_{27}H_{42}O_{20}$ | 685.2191 | Rehmannioside D | 517.1172, 365.1054 | 81720-08-3 |
| 7 | 2.10 | 169.0146 | $[M-H]^-$ | $C_7H_6O_5$ | 169.0137 | Gallic acid | 125.0256 | 149-91-7 |
| 8 | 2.92 | 509.1918 | $[M-H]^-$ | $C_{21}H_{34}O_{14}$ | 509.1870 | Rehmannioside C | 449.1263, 179.0573 | 81720-07-2 |
| 9 | 3.12 | 371.1020 | $[M+Na]^+$ | $C_{15}H_{24}O_9$ | 371.1318 | Ajugol | 191.0596 | 52949-83-4 |
| 10 | 3.69 | 527.1464 | $[M-H]^-$ | $C_{23}H_{28}O_{14}$ | 527.1401 | 6'-O-galloyldesbenzoyl paeoniflorin | 403.0494, 169.0146, 125.0256 | 262350-51-6 |
| 11 | 3.85 | 471.1115 | $[M+Na]^+$ | $C_{19}H_{28}O_{12}$ | 471.1479 | Anacardoside isomer | 309.0966, 125.0504 | 164991-86-0 |
| 12 | 4.21 | 309.0714 | $[M+Na]^+$ | $C_{13}H_{18}O_7$ | 309.0950 | Sakakin | 125.0573 | 21082-33-7 |
| 13 | 4.31 | 125.0504 | $[M+H]^+$ | $C_7H_8O_2$ | 125.0603 | Guaiacol | 110.0286 | 90-05-1 |
| 14 | 4.84 | 417.1438 | $[M-H]^-$ | $C_{22}H_{26}O_8$ | 417.1549 | (-)-Syringaresinol | 181.0548 | 6216-81-5 |
| 15 | 5.10 | 342.1419 | $[M+H]^+$ | $C_{20}H_{23}O_4N$ | 342.1705 | Magnoflorine | 297.0087, 282.0677, 265.0652 | 2141-09-5 |
| 16 | 5.59 | 495.1552 | $[M-H]^-$ | $C_{23}H_{28}O_{12}$ | 495.1508 | Oxypaeoniflorin | 465.1453, 333.1017, 281.0671, 177.0571, 165.0555, 137.0257 | 39011-91-1 |
| 17 | 5.69 | 317.0785 | $[M+H]^+$ | $C_{16}H_{12}O_7$ | 317.0661 | Isorhamnetin | 302.0945 | 480-19-3 |
| 18 | 5.83 | 525.1642 | $[M+HCOO]^-$ | $C_{23}H_{28}O_{11}$ | 525.1608 | Paeoniflorine isomer | 479.1608, 449.1176 | 23180-57-6 |
| 19 | 5.94 | 337.0939 | $[M-H]^-$ | $C_{16}H_{18}O_8$ | 337.0923 | 5-p-coumaroylquinic-acid | 191.0561, 173.0475, 163.0412, 137.0257 | 1899-30-5 |
| 20 | 6.03 | 353.0884 | $[M-H]^-$ | $C_{16}H_{18}O_9$ | 353.0873 | Neochlorogenic-acid | 191.0589, 179.0353, 135.0458 | 906-33-2 |
| 21 | 6.33 | 525.1688 | $[M+HCOO]^-$ | $C_{23}H_{28}O_{11}$ | 525.1608 | Albiflorin | 479.1608, 357.1246, 283.0859, 121,0305 | 39011-90-0 |
| 22 | 6.56 | 711.2562 | $[M-H]^-$ | $C_{33}H_{44}O_{17}$ | 711.2500 | (-) - Syringol-4-o-β- D-carvacosyl - (1 → 2)- β- D-glucopyranoside | 417.1605, 181.0521 | 136997-64-3 |
| 23 | 6.63 | 579.2137 | $[M-H]^-$ | $C_{28}H_{36}O_{13}$ | 579.2078 | (-)-Syringaresinol4-O-β-D- | 449.1481, 417.1563, 181.0493 | 137038-13-2 |

| | | | | | | | | |
|---|---|---|---|---|---|---|---|---|
| | | | | | | glucopyranoside | | |
| 24 | 6.68 | 525.1688 | $[M+HCOO]^-$ | $C_{23}H_{28}O_{11}$ | 525.1608 | Paeoniflorine | 449.1524, 327.1119, 165.0581, 121.0305 | 23180-57-6 |
| 25 | 6.79 | 475.1307 | $[M+HCOO]^-$ | $C_{22}H_{22}O_9$ | 475.1231 | Ononin | 267.0677 | 486-62-4 |
| 26 | 7.28 | 593.1547 | $[M-H]^-$ | $C_{27}H_{30}O_{15}$ | 593.1512 | Quercetin3,7-O-rhamnopyranoside | 447.0977, 301.0397 | 28638-13-3 |
| 27 | 7.29 | 181.0352 | $[M+H]^+$ | $C_9H_8O_4$ | 181.0501 | Theobromine | | 83-67-0 |
| 28 | 7.53 | 447.0938 | $[M+H]^+$ | $C_{22}H_{22}O_{10}$ | 447.1291 | Calycosin-7-O-β-D-glucoside | 285.0525, 270.0334, 213.0376 | 20633-67-4 |
| 29 | 7.53 | 285.0525 | $[M+H]^+$ | $C_{16}H_{13}O_5$ | 285.0763 | Wogonin | 270.0334, 183.0345 | 632-85-9 |
| 30 | 7.56 | 283.0618 | $[M-H]^-$ | $C_{16}H_{12}O_5$ | 283.0607 | Calycosin | 268.0391, 239.0355, 211.0403, 195.0477 | 20575-57-9 |
| 31 | 7.81 | 503.1127 | $[M+Na]^+$ | $C_{23}H_{28}O_{11}$ | 503.1529 | Albiflorin isomer | 341.0789 | - |
| 32 | 8.30 | 465.1453 | $[M-H]^-$ | $C_{22}H_{26}O_{11}$ | 465.1397 | Curculigoside | 327.1082, 204.9773, 123.0461 | 85643-19-2 |
| 33 | 8.38 | 631.1736 | $[M-H]^-$ | $C_{30}H_{32}O_{15}$ | 631.1663 | Galloyl-paeoniflorin | 613.1644, 509.1364, 491.1263, 463.1293 | 122965-41-7 |
| 34 | 8.87 | 711.2562 | $[M-H]^-$ | $C_{33}H_{44}O_{17}$ | 711.2500 | (-)-Syringaresinol4-O-β-D-glucopyranoside isomer | 417.1605, 181.0548 | - |
| 35 | 8.88 | 547.1693 | $[M+Na]^+$ | $C_{21}H_{32}O_{15}$ | 547.1639 | Rehmannioside A isomer | 347.1309 | - |
| 36 | 8.89 | 547.1693 | $[M+Na]^+$ | $C_{26}H_{36}O_{11}$ | 547.2155 | Icariside E3 | 489.1534, 205.0713 | 137822-23-2 |
| 37 | 9.02 | 463.0896 | $[M-H]^-$ | $C_{21}H_{20}O_{12}$ | 463.0877 | Hyperoside | 300.0280, 271.0277, 255.0323, 151.0040 | 482-36-0 |
| 38 | 9.20 | 417.1564 | $[M-H]^-$ | $C_{18}H_{26}O_{11}$ | 417.1397 | Orcinol-1-O-β-D-apiofuranosyl-(1→6)-β-D-glucopyranoside | 109.0280 | 868557-54-4 |
| 39 | 9.22 | 547.1693 | $[M+Na]^+$ | $C_{21}H_{32}O_{15}$ | 547.1639 | Rehmannioside A isomer | 347.1042 | - |
| 40 | 9.24 | 547.1693 | $[M+Na]^+$ | $C_{26}H_{36}O_{11}$ | 547.2155 | Icariside E3 isomer | 489.1670, 205.0831 | - |
| 41 | 9.28 | 301.0006 | $[M-H]^-$ | $C_{14}H_6O_8$ | 300.9984 | Ellagic acide | 283.9997, 229.0150 | 476-66-4 |
| 42 | 9.48 | 623.2043 | $[M-H]^-$ | $C_{29}H_{36}O_{15}$ | 623.1976 | Acteoside | 461.1704, 161.0264 | 61276-17-3 |
| 43 | 9.48 | 623.2043 | $[M-H]^-$ | $C_{29}H_{36}O_{15}$ | 623.1976 | Isoacteoside | 461.1703, 161.0264 | 61303-13-7 |
| 44 | 9.48 | 623.2043 | $[M-H]^-$ | $C_{29}H_{36}O_{15}$ | 623.1976 | Isoverproside | 461.1703, 161.0264 | 61303-13-7 |
| 45 | 9.67 | 939.1226 | $[M-H]^-$ | $C_{41}H_{32}O_{26}$ | 939.1104 | Pentagalloyl-glucose | 617.0902, 465.0791, 295.0512, 169.0146 | 14937-32-7 |
| 46 | 9.73 | 503.1127 | $[M+Na]^+$ | $C_{23}H_{28}O_{11}$ | 503.1529 | Albiflorin isomer | 381.0847, 341.0751, 219.0484 | - |
| 47 | 9.93 | 631.1736 | $[M-H]^-$ | $C_{30}H_{32}O_{15}$ | 631.1663 | Galloylpaeoni-florin isomer | 509.1502, 463.1248, 271.0547 | - |
| 48 | 10.18 | 503.1127 | $[M+Na]^+$ | $C_{23}H_{28}O_{11}$ | 503.1529 | Albiflorin isomer | 381.0887, | - |

| | | | | | | | | |
|---|---|---|---|---|---|---|---|---|
| 49 | 10.48 | 503.1127 | $[M+Na]^+$ | $C_{23}H_{28}O_{11}$ | 503.1529 | Albiflorin isomer | 341.0826, 219.0484 487.1952, 341.1091 | - |
| 50 | 10.86 | 367.0872 | $[M+Na]^+$ | $C_{16}H_{24}O_8$ | 367.1369 | Mudanpioside F | 205.1124 | 172670-08-5 |
| 51 | 10.88 | 163.0412 | $[M-H]^-$ | $C_9H_8O_3$ | 163.0395 | p-Hydroxy-cinnamic acid | 119.0495 | 7400-08-0 |
| 52 | 11.03 | 677.2142 | $[M-H]^-$ | $C_{32}H_{38}O_{16}$ | 677.2082 | Demethylicaritin-7-O-sophoroside | 530.1925, 370.1111 | 101072-83-7 |
| 53 | 11.03 | 677.2142 | $[M-H]^-$ | $C_{32}H_{38}O_{16}$ | 677.2082 | Hexandraside E | 515.1606, 353.1076 | 139955-75-2 |
| 54 | 11.25 | 447.0977 | $[M-H]^-$ | $C_{21}H_{20}O_{11}$ | 447.0933 | Quercetin 3-rhamnoside | 301.0361, 284.0445, 255.0323 | 522-12-3 |
| 55 | 11.60 | 823.2723 | $[M-H]^-$ | $C_{38}H_{48}O_{20}$ | 823.2661 | Rouhuoside | 661.2167, 515.1606, 353.1076 | 131862-37-8 |
| 56 | 11.90 | 523.1858 | $[M-H]^-$ | $C_{21}H_{32}O_{15}$ | 523.2663 | Rehmannioside A | 323.1022, 199.1009 | 81720-05-0 |
| 57 | 12.07 | 793.2632 | $[M-H]^-$ | $C_{37}H_{46}O_{19}$ | 793.2555 | Epimedoside E | 631.2095, 352.0925 | 39049-19-9 |
| 58 | 12.10 | 431.1008 | $[M+H]^+$ | $C_{22}H_{22}O_9$ | 431.1342 | Ononin | 269.0623 | 486-62-4 |
| 59 | 12.11 | 269.0623 | $[M+H]^+$ | $C_{16}H_{13}O_4$ | 269.0814 | Formononetin | 254.0390, 237.0399 | 485-72-3 |
| 60 | 12.17 | 267.0677 | $[M-H]^-$ | $C_{16}H_{12}O_4$ | 267.0658 | Formononetin isomer | 252.0456, 223.0427, 195.0477 | - |
| 61 | 12.41 | 385.0988 | $[M+Na]^+$ | $C_{15}H_{22}O_{10}$ | 385.1111 | Catalpol | 355.1005, 223.0653, 203.0597 | 2415-24-9 |
| 62 | 12.61 | 807.2815 | $[M-H]^-$ | $C_{38}H_{48}O_{19}$ | 807.2712 | Diphylloside B | 661.2220, 645.2285, 499.1685, 514.1526, 353.1076 | - |
| 63 | 12.72 | 661.2167 | $[M-H]^-$ | $C_{32}H_{38}O_{15}$ | 661.2138 | Epimedoside A | 514.1526, 499.1685, 395.1136, 353.1037 | 39012-04-9 |
| 64 | 13.00 | 517.1289 | $[M+Na]^+$ | $C_{19}H_{26}O_{15}$ | 517.1169 | Galloylsucrose | 355.0927 | - |
| 65 | 13.07 | 807.2815 | $[M-H]^-$ | $C_{38}H_{48}O_{19}$ | 807.2712 | Epimedin B | 645.2285, 367.1232, 351.0903, 323.1022 | 110623-73-9 |
| 66 | 13.26 | 385.0988 | $[M+Na]^+$ | $C_{15}H_{22}O_{10}$ | 385.1111 | Catalpol isomer | 355.0889, 223.0683, 203.0656 | - |
| 67 | 13.68 | 629.1945 | $[M-H]^-$ | $C_{31}H_{34}O_{14}$ | 629.1876 | Mudanpioside J | 599.1794, 507.1469, 477.1548, 461.2407 | 262350-52-7 |
| 68 | 13.81 | 485.1012 | $[M+Na]^+$ | $C_{23}H_{26}O_{10}$ | 485.1424 | Lactiflorin isomer | 105.0306 | - |
| 69 | 13.88 | 167.0588 | $[M+H]^+$ | $C_9H_{10}O_3$ | 167.0708 | Paeonol | 149.0061, 124.8925, 121.0297 | 552-41-0 |
| 70 | 13.90 | 485.1012 | $[M+Na]^+$ | $C_{23}H_{26}O_{10}$ | 485.1424 | Lactiflorin | 105.0285 | 1361049-59-3 |
| 71 | 13.95 | 983.3507 | $[M-H]^-$ | $C_{45}H_{60}O_{24}$ | 983.3402 | Acuminatoside | 675.2385, 367.1350, 211.0670 | 142735-71-5 |
| 72 | 13.98 | 485.1103 | $[M+Na]^+$ | $C_{23}H_{26}O_{10}$ | 485.1424 | Lactiflorin isomer | 105.0285 | - |
| 73 | 14.56 | 465.2160 | $[M-H]^-$ | $C_{21}H_{22}O_{12}$ | 465.2130 | Taxifolin-7-O-glucoside | 285.1534, 259.1725, 241.1591 | 14292-40-1 |
| 74 | 14.76 | 477.1047 | $[M+HCOO]^-$ | $C_{21}H_{20}O_{10}$ | 477.1028 | Genistin | 477.1422, 431.0998, | 529-59-9 |

| | | | | | | | | |
|---|---|---|---|---|---|---|---|---|
| 75 | 14.85 | 599.1844 | $[M-H]^-$ | $C_{30}H_{32}O_{13}$ | 599.1770 | Mudanpioside C | 301.0376, 269.0456, 167.7634 569.1843, 477.1458, 281.0706, 165.0581, 137.0257 | 172760-03-1 |
| 76 | 15.34 | 529.1746 | $[M-H]^-$ | $C_{27}H_{30}O_{11}$ | 529.1710 | Icariside I | 367.1232, 309.0795, 297.0454 | 56725-99-6 |
| 77 | 16.24 | 285.0525 | $[M+H]^+$ | $C_{16}H_{13}O_5$ | 285.0763 | Calycosin | 270.0334, 253.0319 | 20575-57-9 |
| 78 | 16.72 | 839.2284 | $[M+H]^+$ | $C_{39}H_{50}O_{20}$ | 839.2974 | Epimedin A | 677.1909, 531.1440, 369.1056, 313.0495 | 110623-72-8 |
| 79 | 16.76 | 675.2385 | $[M-H]^-$ | $C_{33}H_{40}O_{15}$ | 675.2289 | Sagittatoside A | 367.1193, 351.0492, 323,0949 | 118525-35-2 |
| 80 | 17.54 | 839.2284 | $[M+H]^+$ | $C_{39}H_{50}O_{20}$ | 839.2974 | Epimedin A isomer | 677.1855, 531.1440, 369.1056, 313.0458 | - |
| 81 | 17.61 | 675.2385 | [M-H]- | $C_{33}H_{40}O_{15}$ | 675.2289 | Icariin | 529.1887, 513.1673, 367.1232 | 489-32-7 |
| 82 | 18.27 | 645.2285 | $[M-H]^-$ | $C_{32}H_{38}O_{14}$ | 645.2183 | Sagittatoside B | 366.1156, 351.0903, 323.0986 | 118525-36-3 |
| 83 | 19.00 | 823.2366 | $[M+Na]^+$ | $C_{36}H_{48}O_{20}$ | 823.2637 | Jionoside A1 | 677.1909 | 120444-60-2 |
| 84 | 19.05 | 823.2366 | $[M+Na]^+$ | $C_{36}H_{48}O_{20}$ | 823.2637 | Jionoside A1 isomer | 677.1909 | - |
| 85 | 19.12 | 867.3004 | $[M+HCOO]^-$ | $C_{39}H_{50}O_{19}$ | 867.2928 | Baohuoside VI | 659.2437, 366.1156, 351.0903, 323.0949 | 119760-73-5 |
| 86 | 19.14 | 659.2437 | $[M-H]^-$ | $C_{33}H_{40}O_{14}$ | 659.2345 | 2″-O-rhamnosylicarisid e II | 366.1156, 351.0903, 323.0949 | 135293-13-9 |
| 87 | 19.48 | 369.1135 | $[M+H]^+$ | $C_{21}H_{20}O_6$ | 369.1338 | Icaritin | 369.1056, 313.0495, 243.0459, 135.0337 | 118525-40-9 |
| 88 | 19.58 | 513.1826 | $[M-H]^-$ | $C_{27}H_{30}O_{10}$ | 513.1761 | Baohuoside I isomer | 366.1156, 351.0903, 323.0949, 217.0528 | - |
| 89 | 5.99 | 269.0824 | $[M-H]^-$ | $C_{16}H_{14}O_4$ | 269.0808 | Echinatin | 269.1403, 225.1494, 181.1594, 125.0961 | 34221-41-5 |
| 90 | 20.56 | 879.3061 | $[M-H]^-$ | $C_{41}H_{52}O_{21}$ | 879.2923 | Epimedin I | 717.2432, 367.1232 | 205445-00-7 |
| 91 | 22.01 | 531.1926 | $[M-H]^-$ | $C_{27}H_{32}O_{11}$ | 531.1872 | Icaritin-3-O-rhamnopyranoside isomer | 384.1239, 367.1232, 341.1021, 311.0591 | - |
| 92 | 22.43 | 717.2488 | $[M-H]^-$ | $C_{35}H_{42}O_{16}$ | 717.2395 | Sagittatoside C isomer | 513.1873, 367.1232 | - |
| 93 | 22.90 | 687.2371 | $[M+HCOO]^-$ | $C_{29}H_{38}O_{16}$ | 687.2142 | Isomalto-paeoniflorin | 611.2189, 593.1946, 283.0583, 121.0305 | 262350-54-9 |
| 94 | 23.14 | 819.2820 | $[M-H]^-$ | $C_{39}H_{48}O_{19}$ | 819.2712 | Anhydroicaritin-3-O-rhamnoside | 529.1793, 367.1232, | - |

| | | | | | | | | |
|---|---|---|---|---|---|---|---|---|
| | | | | | | (1-2)-furanacid-7-O-glucoside | 289.0951 | |
| 95 | 23.95 | 385.0988 | $[M+Na]^+$ | $C_{15}H_{22}O_{10}$ | 385.1111 | Catalpol | 355.0851, 223.0879, 203.0539 | 2415-24-9 |
| 96 | 24.09 | 269.0623 | $[M+H]^+$ | $C_{16}H_{13}O_4$ | 269.0814 | Formononetin isomer | 254.0390, 237.0399 | - |
| 97 | 24.24 | 829.4650 | $[M+HCOO]^-$ | $C_{45}H_{56}O_{23}$ | 829.4586 | Astragaloside IV | 783.3661 | 84687-43-4 |
| 98 | 24.369 | 821.2583 | $[M-H]^-$ | $C_{39}H_{50}O_{19}$ | 821.2868 | Epimedin C | 659.2068, 366.1078, 351.0942, 323.0654, 311.0627 | 110642-44-9 |
| 99 | 24.43 | 631.2095 | $[M-H]^-$ | $C_{31}H_{36}O_{14}$ | 631.2027 | Demethylanhydroicaritin-3-O-rhamnopyranosyl-xylopyranoside | 352.1002 | - |
| 100 | 24.90 | 499.1639 | $[M-H]^-$ | $C_{26}H_{28}O_{10}$ | 499.1604 | Baohuoside II | 353.1037, 352.0963, 295.1040 | 55395-07-8 |
| 101 | 25.12 | 675.2385 | [M-H]- | $C_{33}H_{40}O_{15}$ | 675.2289 | Icariin isomer | 529.1887, 513.1673, 367.1232 | - |
| 102 | 25.12 | 675.2385 | $[M-H]^-$ | $C_{33}H_{40}O_{15}$ | 675.2289 | Baohuoside VII | 367.1232, 352.1002 | 119730-89-1 |
| 103 | 25.14 | 659.2340 | $[M-H]^-$ | $C_{33}H_{40}O_{14}$ | 659.2340 | 2″-O-rhamnosyl-icariside II | 366.1156, 351.0942, 323.0912 | 135293-13-9 |
| 104 | 25.54 | 659.2345 | $[M-H]^-$ | $C_{33}H_{40}O_{14}$ | 659.2437 | 2″-O-rhamnosyl-icariside II isomer | 366.1156, 351.0903, 323.0949 | - |
| 105 | 25.54 | 479.1330 | $[M+H]^+$ | $C_{23}H_{26}O_{11}$ | 479.1553 | Curculigoside D | 179.0633, 161.0503 | - |
| 106 | 25.71 | 871.4845 | $[M+HCOO]^-$ | $C_{43}H_{70}O_{15}$ | 871.4692 | Astragaloside II | 825.4771 | 84676-89-1 |
| 107 | 25.71 | 871.4845 | $[M+HCOO]^-$ | $C_{43}H_{70}O_{15}$ | 871.4692 | AstragalosideII isomer | 825.4713 | - |
| 108 | 25.74 | 659.2437 | $[M-H]^-$ | $C_{33}H_{40}O_{14}$ | 659.2340 | 2″-O-rhamnosyl-Icariside II isomer | 366.1156, 351.0903, 323.0949 | - |
| 109 | 25.99 | 717.2488 | $[M-H]^-$ | $C_{35}H_{42}O_{16}$ | 717.2395 | Sagittatoside C isomer | 513.1826, 367.1232 | - |
| 110 | 26.20 | 313.0495 | $[M+H]^+$ | $C_{17}H_{12}O_6$ | 313.0712 | Curculigoside A | 151.0317 | 85643-19-2 |
| 111 | 26.21 | 513.1826 | $[M-H]^-$ | $C_{27}H_{30}O_{10}$ | 513.1761 | Baohuoside I | 366.1156, 351.0903, 323.0949, 217.0528 | 113558-15-9 |
| 112 | 26.28 | 913.4961 | $[M+HCOO]^{--}$ | $C_{45}H_{72}O_{16}$ | 913.4797 | Astragaloside I | 867.4873 | 84680-75-1 |
| 113 | 26.58 | 913.4900 | $[M+HCOO]^{--}$ | $C_{45}H_{72}O_{16}$ | 913.4797 | Astragaloside I isomer | 867.4813 | - |
| 114 | 27.03 | 657.2263 | $[M-H]^-$ | $C_{33}H_{38}O_{14}$ | 657.2183 | Anhydroicaritin-3-O-rhamnopyranosyl-furanacid isomer | 513.1826, 367.1193, 352.0963, 289.1229 | - |
| 115 | 27.05 | 913.4961 | $[M+HCOO]^-$ | $C_{45}H_{72}O_{16}$ | 913.4797 | Astragaloside I isomer | 867.4873 | - |

## 2. Components in plasma after KXN administration identified by UPLC/Q-TOF-MS

The preparation of KXN plasma sample is described in the text. Chromatographic condition and Mass spectrum condition UPLC/Q-TOF-MS analysis were consistent with above. The Base Peak Ion (BPI) of KXN plasma in positive and negative ion mode is shown in Supplementary Figure S2.

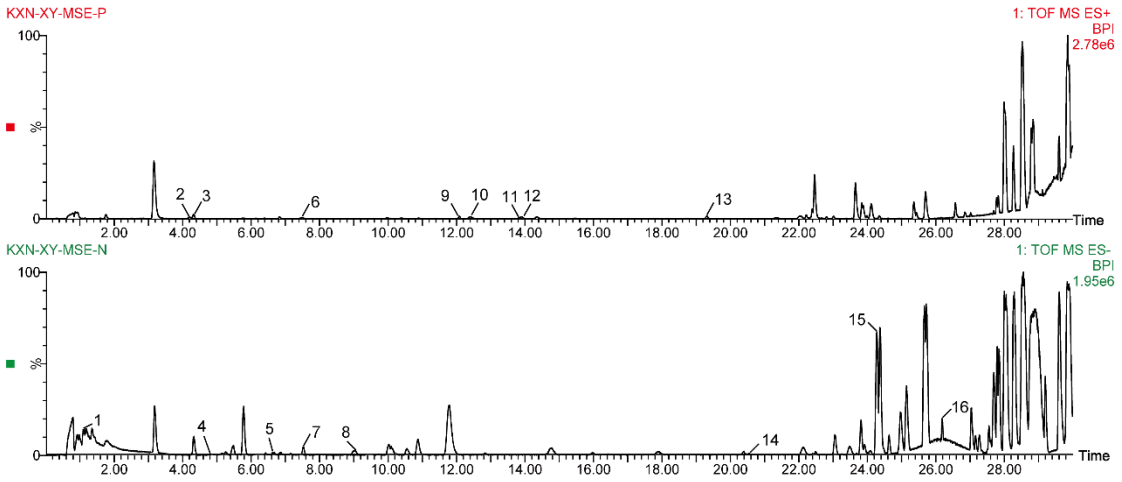


**Supplementary Figure S2.** BPI diagram of KXN plasma UPLC/Q-TOF-MS in positive and negative ion mode.

Combined with molecular network results and Mass spectrometry information comparison, a total of 16 components in plasma of KXN were determined, the specific information is shown in Supplementary Table S2. The mass spectras of each component based on UPLC/Q-TOF-MS are shown in supplementary data sheet S3.

**Supplementary Table S2** 16 absorbable components *in vivo* of KXN

| No. | $t_R$/min | Measured value | Precursor ions | Formula | Theoretical value | Compound | Fragment ion | CAS No. |
|---|---|---|---|---|---|---|---|---|
| 1 | 0.92 | 397.0942 | $[M-H]^-$ | $C_{22}H_{22}O_7$ | 397.1287 | Baohuosu | 268.8040, 259.0176, 191.0193 | 119730-90-4 |
| 2 | 4.30 | 309.0714 | $[M+Na]^+$ | $C_{13}H_{18}O_7$ | 309.0950 | Sakakin | 125.0573 | 21082-33-7 |
| 3 | 4.31 | 125.0504 | $[M+H]^+$ | $C_7H_8O_2$ | 125.0603 | Guaiacol | 110.0286 | 90-05-1 |
| 4 | 4.84 | 417.1438 | $[M-H]^-$ | $C_{22}H_{26}O_8$ | 417.1549 | (-)-Syringaresinol | 181.0548 | 6216-81-5 |
| 5 | 6.68 | 525.1688 | $[M+HCOO]^-$ | $C_{23}H_{28}O_{11}$ | 525.1608 | Paeoniflorine | 449.1524, 327.1119, 165.0581, 121.0305 | 23180-57-6 |
| 6 | 7.53 | 285.0525 | $[M+H]^+$ | $C_{16}H_{13}O_5$ | 285.0763 | Wogonin | 270.0334, 183.0345 | 632-85-9 |
| 7 | 7.56 | 283.0618 | $[M-H]^-$ | $C_{16}H_{12}O_5$ | 283.0607 | Calycosin | 268.0391, 239.0355, 211.0403, 195.0477 | 20575-57-9 |
| 8 | 9.02 | 463.0896 | $[M-H]^-$ | $C_{21}H_{20}O_{12}$ | 463.0877 | Hyperoside | 300.0280, 271.0277, 255.0323, 151.0040 | 482-36-0 |
| 9 | 12.11 | 269.0623 | $[M+H]^+$ | $C_{16}H_{13}O_4$ | 269.0814 | Formononetin | 254.0390, 237.0399 | 485-72-3 |
| 10 | 12.41 | 385.0988 | $[M+Na]^+$ | $C_{15}H_{22}O_{10}$ | 385.1111 | Catalpol | 355.0851, 223.0879, 203.0539 | 2415-24-9 |
| 11 | 15.94 | 167.0588 | $[M+H]^+$ | $C_9H_{10}O_3$ | 167.0708 | Paeonol | 149.0061, 124.8925, 121.0297 | 552-41-0 |
| 12 | 15.89 | 485.1012 | $[M+Na]^+$ | $C_{23}H_{26}O_{10}$ | 485.1424 | Lactiflorin | 105.0285 | 1361049-59-3 |
| 13 | 19.29 | 369.1135 | $[M+H]^+$ | $C_{21}H_{20}O_6$ | 369.1338 | Icaritin | 313.2378, 243.1672, 135.1075 | 118525-40-9 |
| 14 | 20.56 | 879.3061 | $[M-H]^-$ | $C_{41}H_{52}O_{21}$ | 879.2923 | Epimedin I | 717.2432, 367.1232 | 205445-00-7 |
| 15 | 24.24 | 829.4650 | $[M+HCOO]^-$ | $C_{45}H_{56}O_{23}$ | 829.4586 | Astragaloside IV | 783.3661 | 84687-43-4 |
| 16 | 26.21 | 513.1826 | $[M-H]^-$ | $C_{27}H_{30}O_{10}$ | 513.1761 | Baohuoside I | 366.1156, 351.0903, | 113558-15-9 |

| | |
|---|---|
| | 323.0949, 217.0528 |

## 3. OVX model establishment

### 3.1 Surgical Method

The OVX rat model was established using 12-week-old female Sprague-Dawley (SD) rats, weighing 200 – 220 g. The rats were anesthetized using isoflurane via an inhalation system. The surgical area was shaved, sterilized, and disinfected. Two dorsolateral incisions were made to expose the ovaries. After the ovaries were ligated with a surgical line, the ovaries were removed with surgical scissors. The muscle and skin layers were sutured and disinfected. During anesthesia, Duratears Ophtalmic Ointment was applied to prevent corneal drying.

### 3.2 Postoperative Care

Postoperatively, the rats were administered sodium penicillin (5 mg/kg intramuscularly) and ketoprofen (5 mg/kg intramuscularly) for 3 days to prevent infection and manage pain. The rats were closely monitored until they regained consciousness. They were housed at a temperature of 20 – 26°C, with a humidity of 50 ± 10%, and a 12-hour light–dark cycle. Standard rodent diet and water were provided ad libitum.

### 3.3 Assessment Criteria

The success of the OVX model was assessed through several criteria. Specifically, the estrus cycle of ovariectomized rats was observed by vaginal smear on the 4th day after operation, and the ovariectomized model was initially successful with the disturbance of estrus cycle for 5 consecutive days. The blood of castrated rats was collected from posterior orbital venous plexus, and the levels of E2 and FSH in plasma samples were detected by enzyme-linked immunosorbent assay (ELISA). E2 levels were significantly decreased and FSH levels significantly increased as the criteria for successful modeling.

Vaginal lavage cytology of rats after ovariectomy revealed that the blank control group had a higher number of keratinized cells and a lower number of inflammatory cells. In contrast, the ovariectomized group exhibited a marked reduction in keratinized cells and a significant increase in neutrophils. The rats in the model group remained in a persistent diestrus phase, indicating successful initial model establishment (Supplementary Figure S3). Further detection of plasma E2 and FSH levels in the rats showed that the ovariectomized group had significantly decreased plasma E2 levels and significantly increased FSH levels.

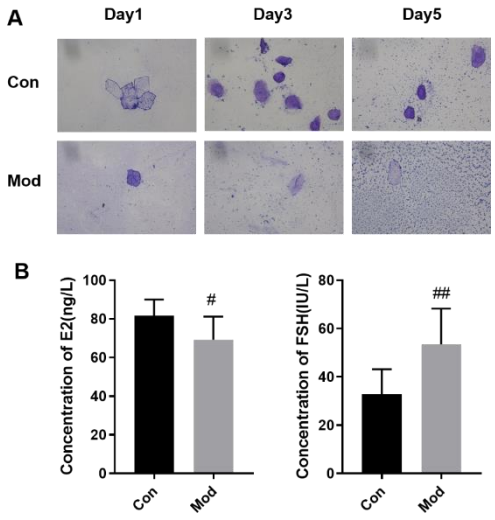


**Supplementary Figure S3.** Modeling evaluation of PMS rats. **(A)** Estrous cycle observation of vaginal douching smear with Wright-Giemsa; **(B)** Plasma E2 and FSH levels were detected by ELISA. Bars represent the Mean ± SD (n = 10). $^{\#}p < 0.05$, $^{\#\#}p < 0.01$ compared with the Con group.

## 4. Proteomic detection procedure in adrenal

### 4.1 Protein Extraction

Samples were first grinded by liquid nitrogen and then the powder was transferred to a 1.5 mL centrifuge tube and sonicated three times on ice, using a high intensity ultrasonic processor in a lysis buffer (8M urea including 1mM PMSF、2mM EDTA). After, the remaining debris was removed by centrifugation at 15000g at 4°C for 10 min. Finally, the protein concentration was determined with a BCA kit according to the instructions of the manufacturer.

### 4.2 Digestion and Cleanup

Equal amount of proteins from each sample were used for tryptic digestion. Add 8M urea to 200ul to the supernatants, then reduced with 10 mM DTT for 45 minutes at 37°C and alkylated with 50 mM iodoacetamide (IAM) for 15 minutes in a dark room at room temperature. 4 × volume of chilled acetone was added and precipitated at -20°C for 2 hours. After centrifugation, the protein precipitate was air-dried and resuspended in 200 μL of 25 mM ammonium bicarbonate solution and 3ul of trypsin (Promega) and digested overnight at 37°C. After digestion, peptides were desalted using C18 Cartridge followed by drying with Vacuum concentration meter, concentrated by vacuum centrifugation and redissolved in 0.1% (v/V) formic acid.

### 4.3 LC-MS/MS Analysis

Liquid chromatography (LC) was performed on a nanoElute UHPLC (Bruker Daltonics, Germany). About 200 ng peptides were separated within 40 min at a flow rate of 0.3 μL/min on a commercially available reverse-phase C18 column with an integrated CaptiveSpray Emitter (25 cm x 75 μm ID, 1.6 μm, Aurora Series with CSI, IonOpticks, Australia).The separation temperature was

kept by an integrated Toaster column oven at 50°C. Mobile phases A and B were produced with 0.1 vol.-% formic acid in water and 0.1% formic acid in ACN. Mobile phase B was increased from 2 to 22% over the first 25 min, increased to 35% over the next 5 min, further increased to 80% over the next 5 min, and then held at 80% for 5 min. The LC was coupled online to a hybrid timsTOF Pro2 (Bruker Daltonics, Germany) via a CaptiveSpray nano-electrospray ion source (CSI).To establish the applicable acquisition windws for diaPASEF mode, the timsTOF Pro2 was operated in Data-Dependent Parallel Accumulation-Serial Fragmentation (PASEF) mode with 4 PASEF MS/MS frames in 1 complete frame. The capillary voltage was set to 1500 V, and the MS and MS/MS spectra were acquired from 100 to 1700 m/z. As for ion mobility range ($1/K_0$), 0.85 to 1.3 Vs/$cm^2$ was used. The "target value" of 10,000 was applied to a repeated schedule, and the intensity threshold was set at 1500. The collision energy was ramped linearly as a function of mobility from 45eV at $1/K_0$ = 1.3 Vs/$cm^2$ to 27 eV at $1/K_0$ = 0.85 Vs/$cm^2$. The quadrupole isolation width was set to 2Th for m/z < 700 and 3Th for m/z > 800.

In diaPASEF mode, the instrument control software was extended to define quadrupole isolation windows as a function of the TIMS scan time. Seamless and synchronous ramping of all applied voltage is achieved by modifying the instrument control electronics. We defined 25 Th isolation windows from m/z about 400 to 1200 and totally 48windows were defined. Other parameters were the same as DDA-PASEF mode.

4.4 Database search and quantification

MS raw data were analyzed using DIA-NN (v1.8.1) with library-free method. the uniprot-proteome_UP000002494_Rat_20220719.fasta database (A total of 46069 sequences) was used to create a spectra library with deep learning algrithms of neural networks. the option of MBR was employed to create a spectral library from DIA data and then reanlyse using this library. The false discovery rate (FDR) of search results was adjusted to < 1% at both protein and precursor ion levels, the remaining identifications were used for further quantification analysis.

**5. Proteomic analysis of the effects of KXN on proteins in OVX rats**

Differences and similarities between the control group (Con), OVX model group (Mod) and KXN administration group (KXN) were evaluated by using OPLS-DA (Supplementary Figure S4). It was found that Mod was significantly separated from the Con group, while KXN group converged toward CON group and separated from Mod group.

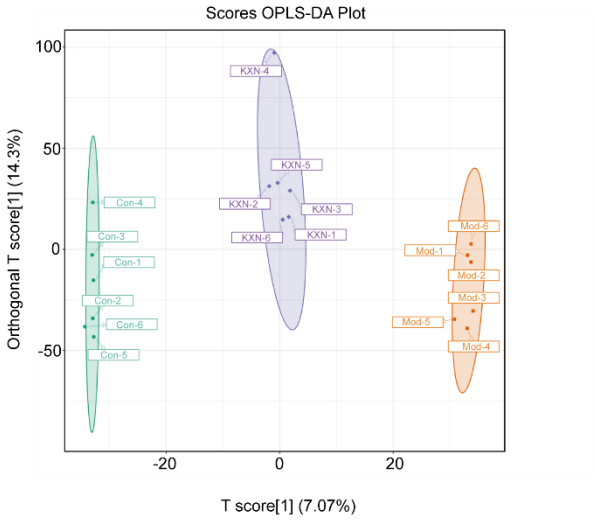


**Supplementary Figure S4.** OPLS-DA plot of the control group (Con), OVX model group (Mod) and KXN administration group (KXN).

Based on OPLS-DA model, peak features that met the screening criteria for both multivariate statistical analysis (VIP > 1) and univariate statistical analysis ($p < 0.05$ and fold change $\geq 1.5$ or $\leq 0.6667$) were selected as the significant differential proteins. The differences in the expression levels of the different proteins in the two groups of samples and the statistical significance of the differences were presented in the volcano maps (Supplementary Figure S5).

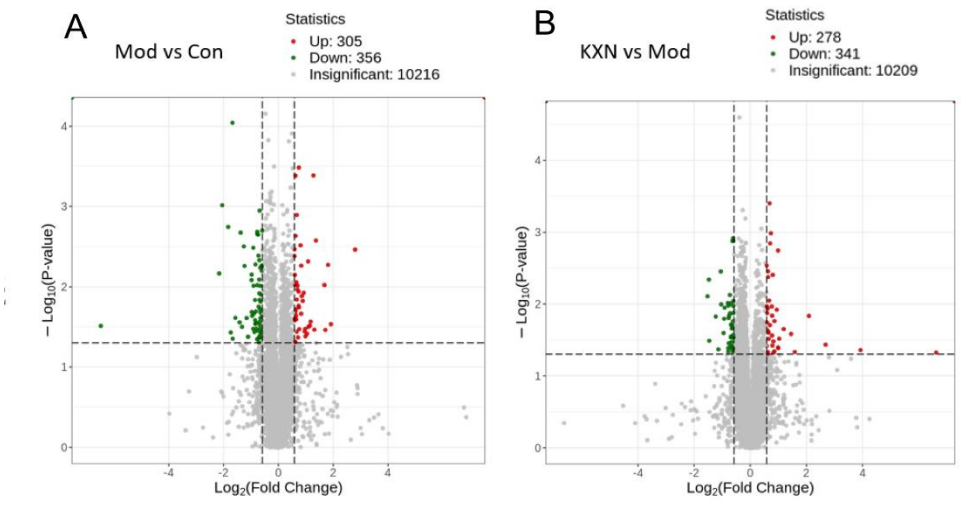


**Supplementary Figure S5. (A)** Volcano diagram depicted the differential expression proteins in OVX model rats versus control rats. **(B)** Volcano diagram depicted the differential expression proteins in KXN administration rats versus OVX model rats. Green, down-regulation; red, up-regulation.

Utilizing z-score normalization of a range of proteins, we generated a clustering heat map to elucidate the expression profiles of distinct proteins across various samples (Supplementary Figure S6).

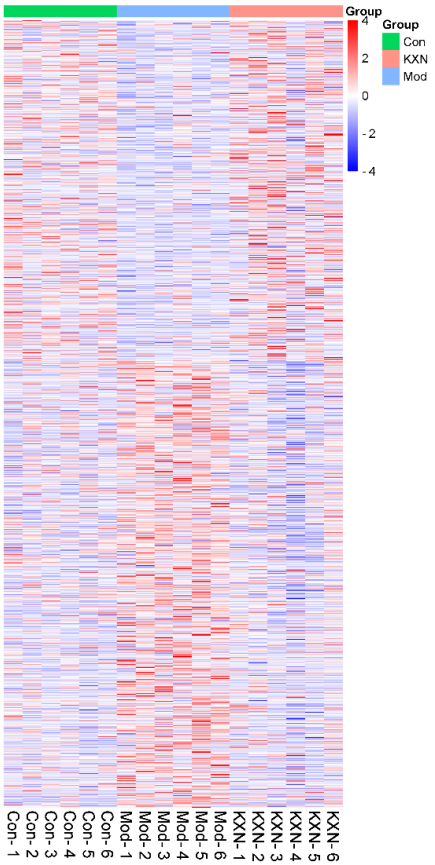


**Supplementary Figure S6.** Heatmap visualized the differentially expressed proteins with $p < 0.05$ and fold change $\geq 1.5$ or $\leq 0.6667$.

## 6. Quantitative analysis of representative associated proteins in steroid hormone biosynthesis pathway

Compared with OVX model group, the expression of HSD3B, CYP21A2, StAR, HSD11B2, which are representative of steroid hormone biosynthesis, was reversed after KXN treatment (Supplementary Figure S7).

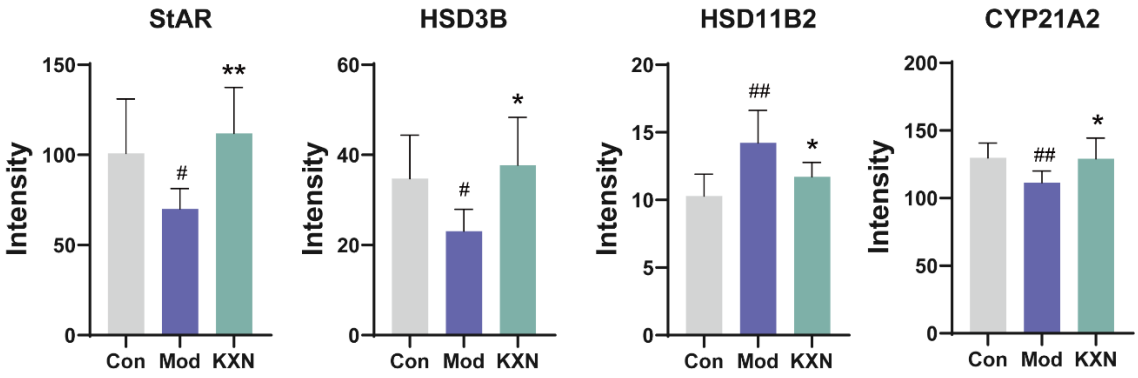


**Supplementary Figure S7.** Quantification of steroid hormone biosynthesis associated proteins detected by adrenal proteomics. Bars represent the Mean ± SD (n = 6). $^{\#}p < 0.05$, $^{\#\#}p < 0.01$ compared with the Con group; $^{*}p < 0.05$, $^{**}p < 0.01$ compared with the Mod group.

## 7. Metabolomics analysis of the effects of KXN on metabolites in OVX rats

The OPLS-DA plot demonstrated a clear separation between the Mod group and the Con group, indicating a significant alteration in either the type or level of metabolites. Following drug intervention, the KXN group exhibited distinct separation from the Mod group, suggesting that KXN effectively regulates metabolic levels in OVX rats (Supplementary Figure S8).

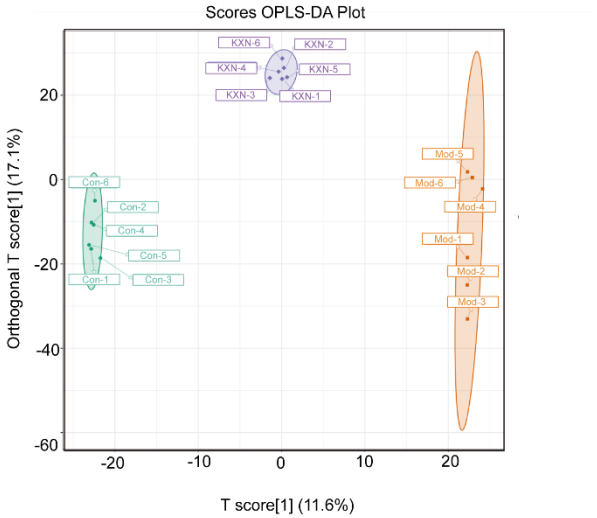


**Supplementary Figure S8.** OPLS-DA plot of the Con, Mod and KXN in metabolomics analysis.

Based on OPLS-DA model, peak features that met the screening criteria for both multivariate statistical analysis (VIP > 1) and univariate statistical analysis ($p < 0.05$) were selected as the significant differential metabolites. The relative content difference of metabolites in the two groups of samples and the statistical significance of the difference are shown in the Volcano Plot (Supplementary Figure S9).

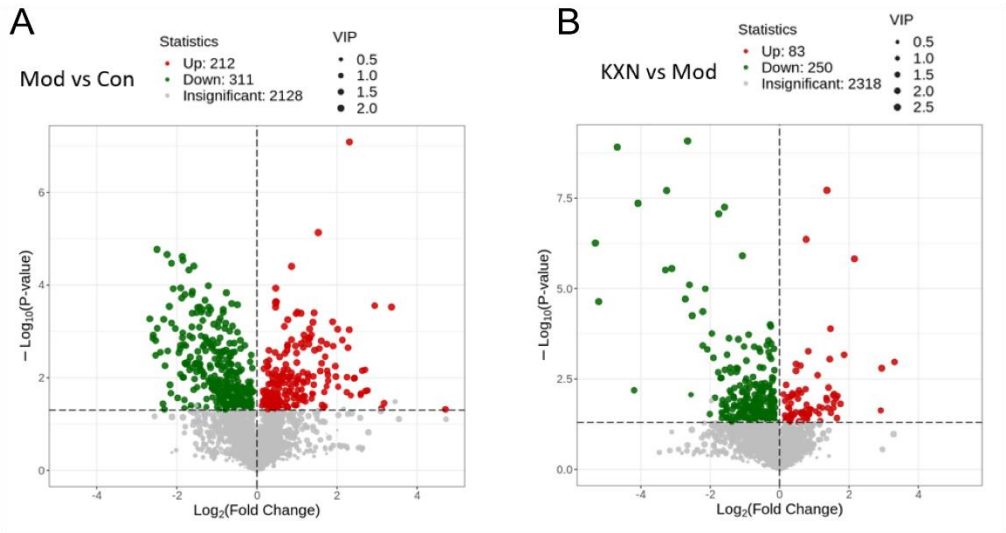


**Supplementary Figure S9. (A)** Volcano diagram depicted the differential metabolites in OVX model rats versus control rats. **(B)** Volcano diagram depicted the differential metabolites in KXN administration rats versus OVX model rats. Green, down-regulation; red, up-regulation.

## 8. The expression of CYP19A1 rat adrenal, uterus, hypothalamus tissues

The expression levels of CYP19A1 in rat adrenal, uterus, hypothalamus tissues were detected by ELISA. The result showed that KXN improve the expression of CYP19A1 in rat adrenal, uterus, hypothalamus tissues (Supplementary Figure S10).

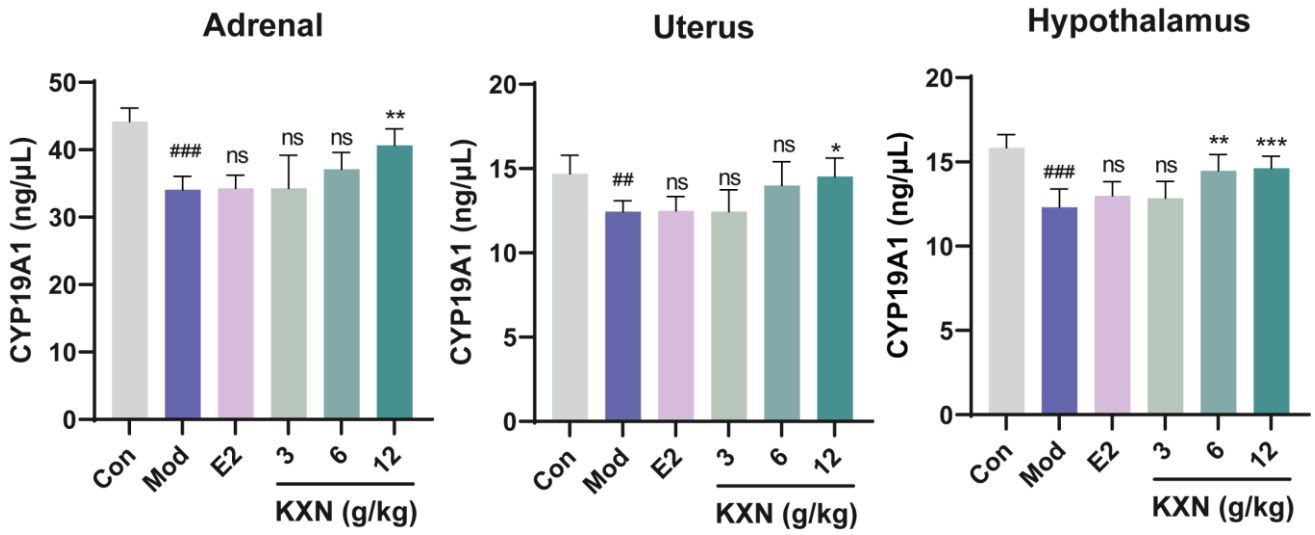


**Supplementary Figure S10.** KXN increase the expression of CYP19A1 in rat adrenal, uterus, hypothalamus tissues. Bars represent the Mean ± SD (n = 6). $^{\#\#}p< 0.01$, $^{\#\#\#}p < 0.001$ compared with the Con group. $^{*}p < 0.05$, $^{**}p < 0.01$, $^{***}p < 0.001$ compared with the Mod group; ns indicates no significant difference compared with the Mod group.

## 9. siRNA-mediated knockdown of CYP19A1 in H295R cells.

A knockdown of CYP19A1 in H295R cells to verify the necessity of CYP19A1 in the mechanism of KXN action. Four siCYP19A1 targeting different gene regions were designed, and WB verification found that SICYP19A1-4 has the best knockdown effect (Supplementary Figure S11A). Treatment with siCYP19A1-4 and other drugs had no effect on cell viability (Supplementary Figure S11B). Notably, after CYP19A1 knockout, the promoting effects of KXN and its three active components (astragaloside IV, icaritin, and baohuoside I) on estradiol secretion were significantly inhibited (Supplementary Material Figure S11C).

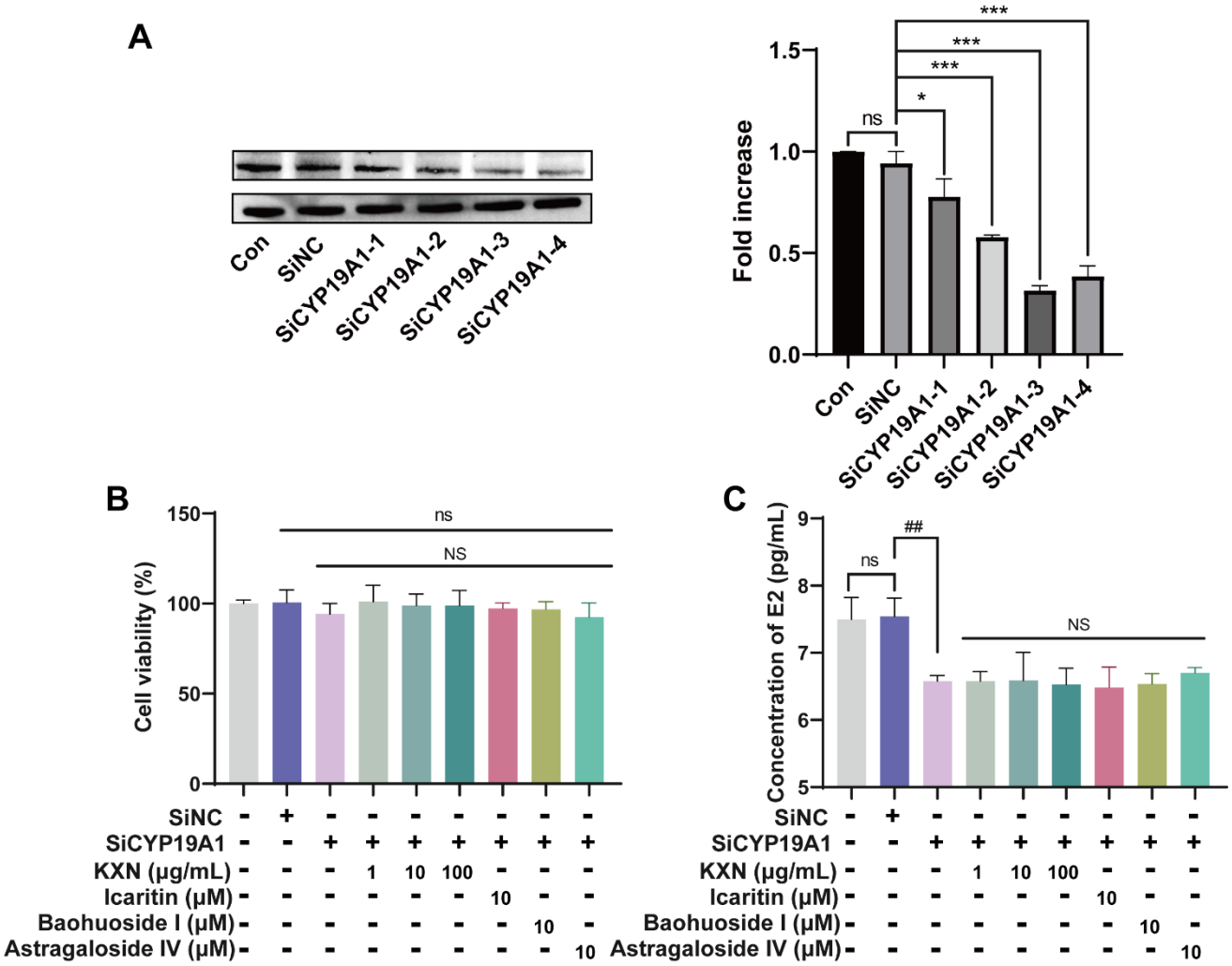


**Supplementary Figure S11.** KXN and its active components were unable to promote estradiol secretion in the absence of CYP19A1. **(A)** The knockout effect of four kinds of SiCYP19A1 in H295R cells by western blot. Bars represent the Mean ± SD (n = 3). ns indicates no significant difference compared with the Con group; $^{*}p < 0.05$, $^{***}p < 0.001$ compared with the SiNC group. **(B)** The cell viability of each group was insignificant after SiCYP19A1 treatmen in H295R cells. Bars represent the Mean ± SD (n = 3). ns indicates no significant difference compared with the Con group; NS indicates no significant difference compared with the SiNC group. **(C)** The promotion effect of KXN and its active components on estradiol secretion was abolished after CYP19A1 knockdown. Bars represent the Mean ± SD (n = 3). ns indicates no significant difference compared with the Con group; $^{\#\#}p < 0.01$ compared with the SiNC group; NS indicates no significant difference compared with the CYP19A1 knockdown group.